Stratospheric Chlorine Injection by Volcanic Eruptions: HCl Scavenging and Implications for Ozone

A. Tabazadeh and R. P. Turco

Because the output of volatile chlorine during a major volcanic event can greatly exceed the annual anthropogenic emissions of chlorine to the atmosphere, the fate of volcanic chlorine must be known. Although numerous observations have shown that volcanoes do not significantly contribute to the stratospheric chlorine burden, no quantitative explanation has been published. Hydrogen chloride (HCl) scavenging processes during the early phases of a volcanic eruption are discussed. A plume dynamics and thermodynamics model is used to show that HCl removal in condensed supercooled water can reduce HCl vapor concentrations by up to four orders of magnitude, preventing substantial stratospheric chlorine injection.

Chlorine emissions during volcanic eruptions have been suggested as a potential cause of global ozone (O_3) depletion (*1*). After the Mount Pinatubo eruption, reduced O_3 concentrations were observed in the tropical stratosphere (*2*). Although the cause of this O_3 depletion has not yet been determined, it may be associated with heterogeneous chemical reactions occurring on the volcanic aerosols (*3*, *4*). Petrologic analysis of Mount Pinatubo (15°N, 120°E) and many other active volcanoes suggests that the abundances of volatile sulfur and chlorine in the eruptive emissions are high. For example, the Mount Pinatubo eruption of June 1991 is estimated to have released about 20 Mt (1 Mt = 1 million metric tons) of SO_2 and 4.5 Mt of HCl (*5*). The El Chichon eruption in April 1982 (17°N, 93°W) may have released about 10 Mt of SO_2 and 1.8 Mt of HCl (*6*). Thus, volcanoes emit large quantities of chlorine into the atmosphere, although the amounts injected into the stratosphere are apparently much smaller (*7*).

The total mass of chlorine in the ambient stratosphere is about 0.5 Mt. A major volcanic eruption may inject 0.5 to 5 Mt of chlorine into the upper atmosphere (*7*, *8*). If most of the emitted chlorine remained in the stratosphere, chlorine concentrations could increase by two to ten times, leading to severe global O_3 depletions. Additional chlorine degassed from the intrusive (noneruptive) magma is not significantly entrained into the explosive plumes that penetrate the stratosphere (*5*, *9*–*12*). The volatile chlorine injected into the troposphere by volcanoes has a short lifetime and is removed by wet deposition processes before it can be transported to the stratosphere.

Ice core data (*13*) show a clear record of sulfur emissions from major historical eruptions. Volcanic SO_2 is converted into sulfate aerosols after injection into the stratosphere. The aerosols are transported to high latitudes in the stratosphere, where they are deposited on ice sheets over a period of several years. Because sulfur has a short lifetime in the lower atmosphere, direct transport in the troposphere can be eliminated as a source of the ice-sulfate, except for cases of local eruptions. Ice core data provide information on the time and magnitude of major eruptions that have disturbed the stratosphere (*14*, *15*). Interestingly, no enhancements in chlorine deposition rates are noted in ice cores after these eruptions (*7*, *13*). In the case of recent eruptions, direct measurements of stratospheric chlorine concentrations indicate that only a small fraction of the emitted chlorine is retained in the upper atmosphere (*16*, *17*). In the case of Mount Pinatubo, less than 1% of the total chlorine emission was detected in the stratosphere (*18*).

It has been suggested that HCl is scavenged by rain induced by volcanic eruptions (*7*, *8*). However, quantitative analysis or calculations have been lacking. The HCl is effectively removed because volcanic plumes contain roughly 1000 times as much water as HCl. The water condenses as the plume cools, and HCl is readily scavenged by liquid water. We use the results from a detailed fluid dynamics–thermodynamics model for volcanic eruption plumes (*19*) to estimate the variations of H_2O, HCl, SO_2, and H_2SO_4 concentrations in a volcanic eruption column. Utilizing these concentration profiles, we show that homogeneous nucleation of H_2SO_4-water aerosols occurs early in the rising column. As the plume continues to loft and cool, these aerosols take up water and are activated into water droplets. Subsequent rapid condensation of water vapor produces liquid water (0.5 to 1.0 g per cubic meter of air) by the time the eruption column reaches the upper troposphere. Dissolution of HCl results in solution droplets that contain 1 to 5% HCl by weight. Correspondingly, HCl gas-phase concentrations in the plume are reduced by up to four orders of magnitude. Alternative HCl removal processes, such as ash surface adsorption, ice crystal absorption and adsorption, and formation of HCl hydrates, are also discussed.

Physical Chemistry of Eruption Plumes

Properties of the eruption column. We used Woods's model (*19*) to predict the temperature, bulk density, and concentrations of gas-phase species as a function of height in an eruption column. This model applies to a Plinian eruption, in which there is continuous discharge of a mixture of gas and solid fragments from a volcanic vent at speeds of hundreds of meters per second. However, a similar dynamical environment can develop during a coignimbrite eruption, in which a rising plume evolves over a dense pyroclastic flow. If the mixture of hot ash and volatiles escaping from the vent entrains and heats a sufficient quantity of ambient air, then the mixture can become buoyant and rise tens of kilometers into the atmosphere. The height reached by such a column depends on the initial temperature and gas mass fraction of the volcanic plume, the vent size, and the total mass of the erupted magma. For given initial conditions at ground level, the fluid dynamics and thermodynamics of gas-solid mixtures determines the velocity, temperature, radius, and density of the ejecta with height in the column (*19*). For initial analysis, the concentration variations of H_2O, HCl, SO_2, and H_2SO_4 were deduced for a vent size of 100 m, an initial temperature of 1000 K, a velocity of 300 m/s, a density of 7.33 kg/m^3 (mixture of ash and gas), and a gas mass fraction of 0.03 (*19*). The results discussed below are not sensitive to these particular parameter values, over a wide range of variation. The eruption plume also contains CO_2, HF, and many other gases, which we have not considered here.

The authors are with the Department of Atmospheric Sciences, University of California, Los Angeles, CA 90024. A. Tabazadeh is also with the Department of Chemistry and Biochemistry, University of California, Los Angeles, CA 90024. R. P. Turco is also with the Institute for Geophysics and Planetary Physics, University of California, Los Angeles, CA 90024.

As the volcanic plume rises, ambient air is entrained and the plume is diluted. The concentrations of trace gases in the plume decrease with altitude accordingly (Fig. 1). To obtain the profiles in Fig. 1, we have assumed that (i) the initial atmospheric pressure at the eruption vent is 1 atm; (ii) the emitted volcanic gas consists of 80% water, 0.5 to 5.0% HCl (low and high cases, respectively), and 0.5 to 5.0% SO_2 by weight; (iii) 1% of the SO_2 is preoxidized to H_2SO_4; and (iv) ambient water vapor is added to the column by entrainment while the other species are simply diluted. The partial pressure of water vapor in the eruption column is strongly dependent on the ambient humidity profile. Figure 1 illustrates the variation with height of the H_2O partial pressure in the volcanic plume corresponding to three standard background humidity profiles, which bracket the extremes of observed humidities (*20*).

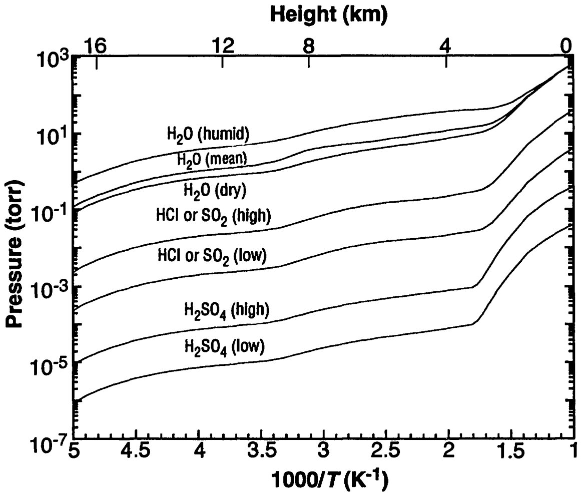

Fig. 1. Partial pressure histories of trace gases in a volcanic eruption plume. The partial pressures are given as a function of the average plume temperature, which decreases monotonically with height from the eruption vent; the height scale, shown on the upper axis, increases from right to left on the chart. Three water vapor curves are shown, corresponding to mean, humid, or dry U.S. Standard Atmosphere ambient water vapor profiles (*20*). These profiles determine the amount of water entrained into the volcanic plume. For illustration, HCl and SO_2 are assumed to have the same initial abundances. The initial H_2SO_4 partial pressure is assumed to be 1% of the initial SO_2 pressure, and SO_2 oxidation in the plume is ignored. We derived the pressure histories using results from the dynamical model of Woods (*19*).

Nucleation and growth of H_2SO_4 aerosol. Although we have assumed that 1% of the SO_2 in the volcanic column is preoxidized into H_2SO_4, the results discussed below are not sensitive to this value within a factor of 10. For the assumed H_2SO_4 concentrations, the high temperatures at the volcanic vent prevent nucleation of sulfuric acid aerosols. However, as the volcanic column rises and cools, the conditions for binary homogeneous H_2SO_4-H_2O nucleation become favorable (*21, 22*).

The rate of aerosol nucleation peaks well above the vent, at about 7 to 9 km. Sulfuric acid–water droplets of about 0.01-μm radius and 80% H_2SO_4 by weight are formed (*22*). As the available H_2SO_4 vapor condenses on these nuclei, the droplets grow by condensation and coagulation to ~0.1-μm radius. Because of the large number of nucleating drops, the coagulation time constant is estimated to be only a few minutes for the initial nuclei (*23*). The concurrent processes of nucleation, condensational growth, and coagulation generate a population of H_2SO_4 particles of ~10^4 to 10^5 per cubic centimeter with an average radius of about 0.1 μm at an altitude of 8 to 12 km in the volcanic column. This evolution of sulfuric acid droplets occurs before the condensation of pure water is possible.

Water vapor condensation. At a sufficient height in the column, the partial pressure of water vapor crosses either the solid-vapor or liquid-vapor phase boundary as shown in Fig. 2. This crossing occurs for all reasonable tropospheric humidity profiles. In the case of a humid background environment (dashed line in Fig. 2), the water vapor partial pressure crosses the water phase transition line near the triple point at a height of about 11 km. When the ambient humidities are lower, water condensation initially favors formation of ice. However, supercooled liquid water is stable at slightly lower temperatures, which are reached almost immediately as the plume rapidly cools. As in convective clouds, ice nucleation is likely to be suppressed until substantial supercooling of an air parcel is achieved (*23*).

Because the volcanic plume is rising and cooling, H_2SO_4-H_2O aerosol droplets nucleated lower in the column take up water vapor, expand in size, and become more dilute. The growth of these aerosols follows a Köhler curve (*4, 24*). As the volcanic column rises from 9 to 14 km, the following effects are predicted to occur: (i) the percent of acid by weight of the droplets decreases from 80% to 10 to 20%; (ii) the number of droplets decreases because of dilution and coagulation from ~10^5 to ~10^4 per cubic centimeter; and (iii) droplet size increases to ~0.2 μm. Water vapor in the column crosses the phase transition boundary at about 14 km (for a typical ambient humidity) (Fig. 2). Freely growing water droplets can form on preexisting sulfuric acid droplets 0.01 to 1 μm in radius when the water vapor supersaturation is roughly 2.0 to 0.2% (*23*). Such supersaturations occur immediately after the ice-phase boundary is crossed, because of the rapid rate of cooling in the buoyant column. Under these conditions, liquid water condensation is favored over ice formation, because ice nucleation typically requires cooling below the frost point by 20°C or more.

The condensation of water vapor continues until its partial pressure in the plume equals the vapor pressure at the local temperature. The amount of water that could condense is indicated for the mean humidity profile in Fig. 2. The condensation of water causes the sulfuric acid aerosols to grow from ~0.2 μm to 4 to 10 μm in radius (for the dry to humid cases, respectively). The total quantity of condensed water at 14 km is about 0.25, 0.50, and 2.7 g/m^3 for the dry, mean, and humid background water vapor profiles, respectively.

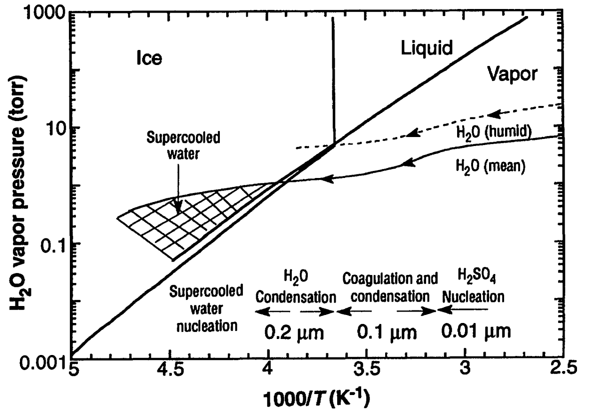

Fig. 2. The variation of the water vapor partial pressure versus temperature (height) in a volcanic eruption plume, superimposed onto the phase diagram of water. The solid line is the water vapor partial pressure history in a volcanic parcel for the case of a mean background humidity profile, and the dashed line, for a humid ambient environment (*20*). The supercooled liquid water vapor pressure line is shown extending from the triple point into the ice region. The potential quantity of condensed supercooled liquid water in the volcanic air parcel is indicated by the hatched region between the water vapor partial pressure history line and the supercooled vapor pressure line. The stages in the evolution of sulfate aerosols in the rising column are shown along the bottom of the chart. Height (and time) increase from right to left.

Scavenging of HCl. The HCl partial pressure in an air parcel rising in a volcanic plume also varies significantly (Fig. 3). Before water begins to condense, HCl is mainly diluted by entrainment of ambient air (hence, following the partial pressure curves in Fig. 1). After water condenses, HCl readily dissolves in the supercooled water to form solutions of approximately 1 to 5% HCl by weight. Dissolution of HCl occurs simultaneously with water vapor condensation; the HCl is quickly partitioned between the vapor and liquid states as water accumulates. At equilibrium, the HCl remaining in the gaseous state is determined by the HCl vapor pressure over a supercooled aqueous solution corresponding to the equilibrium solution composition. In the water-ice region of Fig. 3, where supercooled solutions can exist, the vapor pressure of HCl for a ~1 to 5% HCl solution is in the range of 10^{-6} to 10^{-7} torr. Accordingly, the partial pressure of HCl, initially at 10^{-2} to 10^{-3} torr at the time supercooled water begins to condense, decreases by up to four orders of magnitude as the HCl–water vapor–solution system comes into equilibrium. When water precipitates from the volcanic plume, the dissolved HCl can be removed while the small residual amount of HCl vapor may be injected into the stratosphere. This residual HCl, in the most efficient scavenging case, would contribute only about 0.01% of the total chlorine originally emitted.

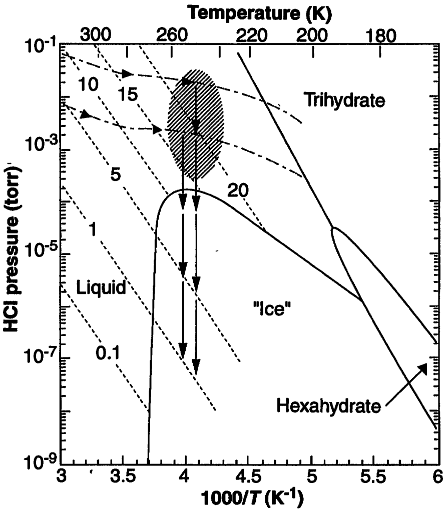

Fig. 3. Partial pressure variations of HCl in an eruption plume (shown as broken lines with arrows in the upper left corner of the chart), superimposed onto the HCl-H_2O vapor pressure phase diagram. The arrows indicate the direction of variation in the HCl partial pressure in the rising column. The shaded region refers to the existence of supercooled water in the eruption column, as determined from Fig. 2. The dashed HCl equilibrium vapor pressure lines correspond to fixed weight percentages of HCl in aqueous solution; the weight percentages are indicated along these lines. For supercooled solutions, the Clausius-Clapeyron relation is used to extend the vapor pressure lines into the "ice" region. The HCl hexahydrate stability region is roughly defined in the lower right corner of the plot. Data that define the phase boundaries were taken from (*25*) and (*31*).

Without HCl uptake by supercooled water, the HCl partial pressure would remain high enough ($>10^{-4}$ torr) that the HCl-H_2O trihydrate could eventually form (Fig. 3). The potential contribution of HCl hydrates to chlorine scavenging is discussed below.

Dissolution of SO_2. Sulfur dioxide also dissolves in water according to the approximate relation

$$[SO_2] = (K_1 K_H P_{SO_2})^{1/2}$$

where $[SO_2]$ is the aqueous concentration of SO_2, K_1 is the first dissociation constant of H_2SO_3, K_H is Henry's constant for SO_2 dissolution (*26*), and P_{SO_2} is the partial pressure of SO_2 over the solution. For the conditions of interest (temperature of ~235 K at an altitude of 14 km in the volcanic column), Henry's constant has a value of about K_H = 21.6 M/atm (M = moles per liter), and the first dissociation constant is about K_1 = 0.08 M. The partial pressure of SO_2 can vary from 10^{-2} to 10^{-3} torr (see Fig. 1), which leads to SO_2 concentrations of about 0.0015 to 0.0050 M. With 0.5 g/m^3 of condensed water present, only about 0.5 to 1.5% of the SO_2 in the plume would be removed by SO_2 dissolution. Thus, supercooled water selectively scavenges HCl relative to SO_2 from the vapor phase.

Other HCl Removal Mechanisms

Ash scavenging. Rose (*9*) analyzed the chemical composition of volcanic ashfall and estimated that roughly 10 to 20% of the emitted HCl may be scavenged on mineral particle surfaces that fall out of the volcanic cloud. Such scavenging might be related to the condensation of water vapor on ash surfaces, with dissolution of HCl in the water (*9*) or collection of dilute H_2SO_4 droplets containing HCl by the ash. The acidic chlorine could remain on the ash, perhaps as chloride salts, such as NaCl, after the water had evaporated (*9*). Nevertheless, the measured scavenging of chlorine by volcanic ash is on the order of magnitude too small to account for the stratospheric observations (*16, 18*).

As water vapor condenses in the column, the surfaces of ash particles may become coated by a layer of ice. The HCl is strongly adsorbed onto ice surfaces, which may become completely coated at low temperatures (*27, 28*). The total mass of HCl that might be adsorbed onto ice-coated ash may be estimated as

$$M_{HCl} = n_s S_{ash} m_{HCl}$$

where n_s is the total number of sites for adsorption per unit area of ice surface, which is approximately 10^{15} sites per square centimeter (*29*), S_{ash} is the total surface area of the ash, and m_{HCl} is the molecular mass of HCl in grams. If the ash is completely covered with a monolayer of HCl, then 1 cm^2 of ash surface can remove 10^{15} HCl molecules from the gas phase. The surface area-to-volume ratio of ash particles may be approximated with an r^{-1} dependence, where r is appropriately averaged over the particle size distribution. Using the r^{-1} dependence for the surface area-to-volume ratio and assuming a specific density of ash of about 3.0 g/cm^3, we find that the adsorbed mass of HCl is given approximately as

$$\frac{M_{HCl}}{M_{ash}} = \frac{6.1 \times 10^{-8}}{r}$$

where M_{ash} is the total ash mass, M_{HCl} is the total mass of adsorbed HCl, and r is in centimeters.

In volcanic eruptions, the total mass of ash is roughly ten times the total mass of emitted water. The total mass of emitted water is roughly 100 times the total mass of emitted HCl (*5, 6*), although the water burden in the plume may be further increased by a factor of 10 or more through entrainment of ambient water vapor. These estimates of the relative amounts of ash, water, and HCl are reasonable for the recent eruptions of Mount Pinatubo and El Chichon (*5, 6*). Hence, if the radius of the ash particles in the volcanic clouds were 10 μm, the ash surfaces could scavenge about 6% of the total HCl (where M_{ash} is assumed to be 1000 M_{HCl}). If the effective ash particle radius were 1 μm, up to 60% of the HCl could be scavenged. Thus, although it is possible to achieve a factor of 2 depletion of volatile chlorine from the plume, HCl scavenging efficiencies of 99% or more are not likely for ice-coated mineral ash.

Scavenging of HCl on clean ash surfaces is even less likely. Studies of HCl adsorption on glass, for example, show that only a small amount of HCl can be taken up (*30*). Unless the silicate ash surfaces are reactive toward HCl at temperatures below ~300 K, the overall scavenging of volatile chlorine by ash should be limited to ~10%, as observed (*9*).

Formation of ice crystals. The solubility of HCl in bulk ice is only of the order of 10 parts per million by volume, or mole fractions of about 10^{-5} to 10^{-6} (*31–33*). Because the mass ratio of H_2O to HCl in the volcanic plume is ~100:1 to 1000:1, removal of HCl by dissolution in ice cannot be significant. Nevertheless, ice crystals may scavenge HCl on their surfaces. At rapid rates of condensation and freezing, water saturated with HCl might trap HCl within bulk inclusions. For an ice density of 1.0 g/cm^3, the mass of HCl that could be adsorbed on ice crystal surfaces is

$$\frac{M_{HCl}}{M_{ice}} = \frac{1.8 \times 10^{-7}}{r}$$

where M_{ice} is the total mass of ice formed (consisting of emitted and entrained water). For an average ice crystal radius of 10 μm, the ice surfaces could scavenge about 2 to 20% of the HCl (M_{ice} = 100 to 1000 M_{HCl}). Typical cirrus clouds contain ice crystals with sizes of 10 to 100 μm. Hence, HCl removal on ice surfaces would logically account for 10% or less of the total volatile chlorine, although a factor of 10 reduction may not be ruled out in the extreme case of high concentrations of small ice crystals (which might not fall out of the plume, however).

Hydrates of HCl. As already noted, HCl is highly soluble in liquid water but is not soluble in ice. However, if the HCl concentration in an aqueous solution becomes large enough, HCl trihydrate or hexahydrate crystals can precipitate from the solution. The direct formation of these HCl hydrates from the vapor phase is unlikely for two reasons. First, as seen in Fig. 3, the stability region for HCl hydrates is far removed from the actual conditions present in the volcanic plume. Second, because supercooled water is generated early in the plume evolution, HCl vapor is strongly depleted by dissolution in the water, further hindering hydrate formation.

If HCl vapor were not scavenged by dissolution in supercooled water, then the trihydrate stability regime would be reached at HCl partial pressures of ~10^{-3} to 10^{-2} torr at a temperature of ~210 to 220 K (Fig. 3). However, formation of hydrates, if it occurred, would not be capable of strongly reducing the HCl partial pressure unless there were deep sustained cooling of the plume. Moreover, it is improbable that hydrates would form. The equilibrium vapor pressure of water over ice at this point in the eruption column is approximately 0.01 to 0.1 torr. Under these conditions, the formation of HCl-H_2O liquid solutions is still thermodynamically favorable (*31*). That is, if the HCl had not been removed earlier by dissolution in supercooled water, then it could simultaneously condense with water vapor to form more concentrated HCl-H_2O solutions (~10% HCl by weight). The hexahydrate is less likely to condense in the eruption column than the trihydrate, because the maximum temperature for hexahydrate formation is roughly 200 K (Fig. 3). These low temperatures occur in the eruption column at high altitudes close to the stabilization point, implying further dilution of HCl in the column. The probability of HCl hydrate formation directly from the gas phase is thus improbable for the conditions found in an eruption column.

Thermochemistry at the vent. It is possible that HCl vapor in the volcanic column might interact with ash particles at high temperatures near the eruption vent and directly form refractory chloride salts. However, thermochemical calculations have shown that HCl is by far the most stable form of chlorine under eruptive conditions (*34*). Accordingly, the scavenging of HCl by thermochemical processes is unlikely. Measurements of ash composition place further limitations on the efficiency of thermochemical reactions, inasmuch as less than 20% of the emitted chlorine is recovered as soluble chloride residue on ash fallout (*9*).

Stratospheric Implications

After analyzing the physical chemistry, thermodynamics, and microphysics of a volcanic eruption column, we conclude that HCl is removed from volcanic eruption plumes primarily by dissolution in liquid water droplets, followed by rainout or collection of the droplets by falling debris. These water droplets condense on aerosols nucleated in the rising column from emitted sulfuric acid vapor. Airborne measurements in volcanic clouds and reports of rainfall associated with volcanic eruptions support this conclusion. Aerosol samples collected during and immediately after eruptions show the presence of large numbers of dilute sulfuric acid droplets (*35–37*). The rain that follows most large eruptions is clearly a result of water condensation in the eruption column (*8*), although the microphysical mechanisms have not been resolved. This water readily scavenges HCl and may account for the absence of large stratospheric chlorine injections accompanying major volcanic eruptions. Measurements of chloride and sulfate in the rainfalls induced by volcanic eruptions may shed some light on the processes described above.

Several recent volcanic eruptions have emitted as much as 0.5 to 5.0 Mt of HCl, which is equivalent to two to ten times the total background stratospheric chlorine burden. Dissolution appears capable of reducing HCl vapor concentrations in volcanic plumes by up to four orders of magnitude. If the dissolution mechanism proposed here is efficient, then the fractional amount of volcanic HCl vapor injected into the stratosphere will always be 1% or less of the total volatile chlorine emitted. After the Mount Pinatubo eruption, which released ~4.5 Mt of HCl, global chlorine abundance in the stratosphere increased by less than ~1% (*16, 18*), consistent with efficient scavenging of the volcanic chlorine. If the supercooled water dissolution mechanism were inefficient, other processes might remove ~10 to 90% of the emitted chlorine. Still, 10% or more would remain in the stratosphere. In the cases of Mount Pinatubo and El Chichon, stratospheric chlorine concentrations could have roughly doubled, causing significant global O_3 reductions. Such putative increases in stratospheric chlorine after major eruptions are not observed either recently (*16, 18*), or in the historical record of chlorine deposition in ice cores (*13*).

After the eruption of El Chichon in 1982, an enhancement of about 3% in the total stratospheric HCl burden was detected (*38*). This increase is believed to be associated with the unusual mechanical entrainment and injection of halite evaporites, mainly NaCl, which reacted in the stratosphere with H_2SO_4 to produce HCl (*39*). The halite reaction occurred over a period of 2 months and thus created a delayed source of stratospheric HCl. On the basis of similarities between the Mount Pinatubo and El Chichon eruptions, we expect that direct HCl injection by El Chichon accounted for only a small fraction of the observed stratospheric chlorine increase.

The stratospheric O_3 layer is, it seems, protected from the chlorine vapors emitted by volcanoes. However, the efficiency of chlorine removal may be sensitive to environmental conditions, such as ambient humidity and tropopause temperature and height. Further studies of the physical and chemical mechanisms operating in volcanic eruption columns and of the prompt fallout from volcanic clouds should be carried out to resolve uncertainties in the volcanic source of chlorine. Finally, our results contradict some assertions (*1*) that chlorine present in the stratosphere (and affecting O_3) is provided in large part by volcanic eruptions and not by industrially manufactured chlorofluorocarbons.

REFERENCES AND NOTES

1. D. A. Johnston, *Science* **209**, 491 (1980).
2. W. B. Grant *et al.*, *Geophy. Res. Lett.* **19**, 1109 (1992).
3. M. Prather, *J. Geophys. Res.* **97**, 10187 (1992).
4. R. P. Turco and P. Hamill, *Ber. Bunsenges. Phy. Chem.* **96**, 323 (1992).
5. H. R. Westrich and T. M. Gerlach, *Geology* **20**, 867 (1992).
6. J. C. Varekamp, J. F. Luhr, K. L. Prestegaardd, *J. Volcanol. Geotherm. Res.* **23**, 39 (1984).
7. J. P. Pinto, R. P. Turco, O. B. Toon, *J. Geophys. Res.* **94**, 11165 (1989).
8. A. L. Lazrus *et al.*, *ibid.* **84**, 7869 (1979).
9. W. I. Rose, *Geology* **5**, 621 (1977).
10. A. T. Anderson, *Geol. Soc. Am. Bull.* **85**, 1485 (1974).
11. P. S. Taylor and R. E. Stoiber, *ibid.* **84**, 1031 (1973).
12. G. J. Bluth *et al.*, *Geophys. Res. Lett.* **19**, 151 (1992).
13. R. J. Delmas, *Rev. Geophys.* **30**, 1 (1992).
14. M. Legrand and R. J. Delmas, *Atmos. Environ.* **18**, 1867 (1984).
15. S. Kirchner and R. J. Delmas, *Ann. Glaciol.* **10**, 80 (1988).

16. L. Wallace and W. Livingston, *Geophys. Res. Lett.* **19**, 1209 (1992).
17. A. L. Lazrus *et al.*, *J. Geophy. Res.* **81**, 1067 (1976).
18. M. G. Mankin, M. T. Coffey, A. Goldman, *Geophys. Res. Lett.* **19**, 179 (1992).
19. A. W. Woods, *Bull. Volcanol.* **50**, 169 (1988).
20. "U.S. Standard Atmosphere" (Government Printing Office, Washington, DC, 1976).
21. J. Zhao and R. P. Turco, in preparation.
22. P. Hamill *et al.*, *ibid.* **13**, 561 (1982).
23. R. R. Rogers and M. K. Yau, *A Short Course in Cloud Physics* (Pergamon, Oxford, ed. 3, 1989); H. R. Pruppacher and J. D. Klett, *Microphysics of Clouds and Precipitation* (Reidel, Dordrecht, Holland, 1978).
24. H. M. Steele and P. Hamill, *J. Aerosol. Sci.* **12**, 517 (1981).
25. M. J. Molina, in *CHEMRAWN VII*, J. G. Calvert, Ed. (Blackwell, Oxford, in press).
26. D. R. Schryer, *Heterogeneous Atmospheric Chemistry* [*Geophys. Monogr. 26, Am. Geophys. Union* (1982)], p. 187.
27. D. R. Hanson and A. R. Ravishankara, *J. Phys. Chem.* **96**, 2682 (1992).
28. A. Tabazadeh and R. P. Turco, *J. Geophys. Res.*, in press.
29. A. W. Adamson, *Physical Chemistry of Surfaces* (Wiley, New York, ed. 5, 1990).
30. M. T. Leu, *Geophys. Res. Lett.* **15**, 851 (1988).
31. D. R. Hanson and K. Mauersberger, *J. Phys. Chem.* **94**, 4700 (1990).
32. J. Marti and K. Mauersberger, *Geophys. Res. Lett.* **18**, 1861 (1991).
33. S. Elliott *et al.*, *ibid.* **17**, 425 (1990).
34. R. B. Symonds, M. H. Reed, W. I. Rose, *Geochim. Cosmochim. Acta* **56**, 633 (1992).
35. D. B. Smith *et al.*, *J. Geophys. Res.* **87**, 4963 (1982).
36. W. I. Rose, R. L. Ghuan, D. C. Woods, *ibid.*, p. 4956.
37. W. I. Rose *et al.*, *Am. J. Sci.* **280**, 671 (1980).
38. W. G. Mankin and M. T. Coffey, *Science* **226**, 170 (1984).
39. D. C. Woods, R. L. Chuan, W. I. Rose, *ibid.* **230**, 170 (1985).
40. We thank W. Rose for helpful discussions, T. Gerlach and H. Westrich for a preprint of their manuscript on Mount Pinatubo, and J. Zhao for providing us with her nucleation code. This work is supported by the National Aeronautics and Space Administration (NASA) Upper Atmosphere Program under grant NAGW-2183 and the National Science Foundation Atmospheric Chemistry program under grant ATM-8911836. A.T. was supported by a NASA Fellowship in Global Change Research under grant NGT-30079.

On the Crawling of Animal Cells

Thomas P. Stossel

Cells crawl in response to external stimuli by extending and remodeling peripheral elastic lamellae in the direction of locomotion. The remodeling requires vectorial assembly of actin subunits into linear polymers at the lamella's leading edge and the crosslinking of the filaments by bifunctional gelation proteins. The disassembly of the crosslinked filaments into short fragments or monomeric subunits away from the leading edge supplies components for the actin assembly reactions that drive protrusion. Cellular proteins that respond to lipid and ionic signals elicited by sensory cues escort actin through this cycle in which filaments are assembled, crosslinked, and disassembled. One class of myosin molecules may contribute to crawling by guiding sensory receptors to the cell surface, and another class may contribute by imposing contractile forces on actin networks in the lamellae.

Ungainly in comparison to flying, swimming, or running, the crawling motions of single animal cells are nevertheless profoundly important. Countless foraging ameboid cells creep through the soil and beneath the waters, and movements of single cells are fundamental for the life of multicellular beings. After conception, selected cells of the developing mammalian zygote invade the uterine wall to establish the placenta, while the intricately programmed migration of other cells within the embryo shapes the complex form of the emerging organism. Legions of white blood cells patrol body tissues to engage hostile microorganisms. Locomotion of fibroblastic and epithelial cells heals wounds, and osteoblasts and osteoclasts crawl about as they remodel bone. The crawling malignant tumor cells that invade and disrupt normal tissue architecture account as much or more for the lethality of cancer than does uncontrolled growth. The wiring of the nervous system during fetal development takes place when peripheral segments of neuronal cells crawl, stretching out dendrites and axons; as delicate processes, the axons can extend for enormous distances. Related functionally to crawling are phagocytosis and cell spreading. The latter permits tissue macrophages and lymphocytes to grasp one another as they process antigens to program specific immune responses. Motions analogous to crawling also transform blood platelets from smooth disks to spiny spheres that plug vascular leaks after injury.

Research programs directed at describing cell crawling behavior are on a collision course with studies investigating the molecular aspects of sensory and motor machinery, but the richness of detailed information emerging from these investigations can obscure their interrelationships. This article aims to integrate these programs, based on the optimistic view that, despite large information gaps, it is reasonable to speculate on how cells crawl. Emphasized is one of the most difficult and confusing aspects of the crawling mechanism: the role of the self-assembling protein actin in the cell surface rearrangements that accompany crawling (*1*).

Crawling

Cells initiate crawling in response to surface stimulation, usually in the form of soluble or substrate-bound extracellular molecules that act as sensory cues. The agonists, which include proteins, peptides, lipids, and small molecules, bind to specific externally disposed receptors. These sensors may be of the serpentine type coupled to heterotrimeric guanosine triphosphate (GTP)–binding protein (G protein), which pass repeatedly through the membrane, single-spanning proteins with tyrosine kinase activities in their cytoplasmic tails, or even receptors linked to the outer membrane leaflet by glycolipid anchors with no obvious direct connections to intracellular components (*2*). Less specific physical perturbations of the plasma membrane, such as exposure of cells to electrical fields, positively charged beads, or mechanical distortions, can also produce crawling behavior (*3*). The interaction of sensory influences with the membranes of cells initiates transmembrane signals that activate the complex machinery of crawling (*4*).

The crawling cell invariably has a polarity, the most conspicuous feature of which is leading lamellae, thin veillike structures that are free of organelles visible in the light microscope and that extend from the organelle-rich cell body in the direction of movement (*5*) (Fig. 1A). The lamellae, which may have smooth or serrated anterior edges, appear to glide forward, pulling the cell body passively behind them. As the lamellae advance, they consolidate their forward progress by transient attachment to the underlying surface. Thus, the crawling machinery requires, in addition to the restructuring of the peripheral substance of cells, reversible adhesion of externally disposed plasma membrane molecules to the substrate along which the cell crawls (*6*).

Cells put out variable numbers of lamellae, but only lamellae that contact the substrate on which the cells are crawling are capable of generating locomotion. Of these, usually one becomes dominant in an actively crawling cell. As the dominant lamella expands, the others withdraw coordinately. Contractions at the junction of the lamella and the cell body and also at the rear of the cell deform the cell body and

---

The author is with the Division of Experimental Medicine, Brigham and Women's Hospital, Department of Internal Medicine, Harvard Medical School, Boston, MA 02115.